NJC

PAPER

View Article Online
View Journal | View Issue

Cite this: *New J. Chem.*, 2014, **38**, 4235

Non-symmetric dimers comprising chalcone and cholesterol entities: an investigation on structure–property correlations†

Ammathnadu S. Achalkumar,*[a] Doddamane S. Shankar Rao[b] and Channnabasaveshwar V. Yelamaggad*[b]

Received (in Montpellier, France) 21st March 2014,
Accepted 20th May 2014

DOI: 10.1039/c4nj00426d

www.rsc.org/njc

Four series of new dimers formed by interlinking chalcone and cholesterol mesogenic entities through spacers of varying length and parity have been synthesized and characterized by polarizing optical microscopy, differential scanning calorimetry, X-ray diffraction and electrical switching studies. The structure of the chalcone core has been systematically modified to investigate the effect of the molecular structure on the thermal behaviour of the dimers. The study demonstrates the dramatic dependence of thermal behaviour of these dimers on the nature of the chalcone as well as the length and parity of the spacer.

I. Introduction

Liquid crystal (LC) phases formed by the self-assembly of shape anisotropic molecules (mesogens) represent a distinct and unique state of matter.[1] Since their discovery[2] they have attracted attention as they combine the order of solids and the mobility of liquids at the molecular and mesoscopic levels.[1] The chiral LC phases, resulting from entirely chiral mesogens or by doping the LC phase with a suitable chiral dopant, are fascinating as they exhibit novel structures and special properties that are promising in the arenas of both basic and applied research.[3–5] The helical superstructures of the chiral nematic (N*) or chiral smectic C (SmC*) phases have been recognized as media for device applications,[3] and frustrated phases such as blue phases (BPs) and twist grain boundary (TGB) phases have generated great interest owing to their complex structures.[4,6] Three types of blue phases *viz.*, BPI, BPII and BPIII are known to exist which comprise double twist cylinders, as shown in Fig. 1a. Generally, BPs exist over a short thermal range between the N*/smectic (Sm) phase and the isotropic liquid (I) phase. Owing to their huge promise in transmissive[6a,b] and reflective displays,[6c–e] and photonics applications,[6f–i] there have been efforts to widen the thermal stabilities of these phases.[6j,k] Similar to BPs, TGB phases occur over a short thermal range at the phase transition from the I/N* to smectic A (SmA) or chiral smectic (SmC*) phases. Although their importance in applied science is not revealed hitherto, they have attracted attention being regarded as LC analogues of the Abrikosov phases exhibited by type-II superconductors. Three main types of TGB phases are the TGBA, TGBC and TGBC* where the slabs have orthogonal smectic A (SmA), tilted smectic C (SmC) and helical SmC* characters respectively. As representative cases, the structures of TGBA and TGBC* are shown in Fig. 1d and e.

In recent years, liquid crystalline dimers composed of either two identical (symmetrical) or non-identical (non-symmetrical) mesogens interlinked through a flexible spacer have been intensively investigated, not only because they serve as model systems for polymeric LCs but also due to their remarkable thermal behaviour exhibiting an odd–even effect, new LC phases, unprecedented phase sequences, frustrated phases *etc.*[7–15] For example, symmetric dimers are known to exhibit a rich smectic polymorphism besides showing an archetypal spacer-parity directed odd-effect.[7] Recently, one of the most remarkable phase transition properties of such symmetric, achiral dimers with an odd-numbered spacer has been disclosed;[8] the occurrence of a new twist-bend nematic (N_{tb}) phase, which signifies a structural correlation among the well-known uniaxial nematic (N) and the N* phases, has been reported (Fig. 1f–h). Notably, this new nematic order is non-layered, polar and structurally chiral, although the constituent mesogens themselves are achiral. In fact, in this phase, the constituent molecules self-assemble to form a helical structure and unlike in the N* phase, the local director (**n**) (a preferred orientational direction of mesogens) is not perpendicular to the helix axis but forms an angle that depends on the magnitude of the spontaneous bend and the twist elastic constant. Interestingly, there has been speculation about the correlation between the N_{tb} structure and double-twist structure of the BPs formed by

[a] *Indian Institute of Technology Guwahati, Guwahati, 781039, Assam, India. E-mail: achalkumar@iitg.ernet.in*
[b] *Centre for Soft Matter Research, Jalahalli, P. B. No. 1329, Bangalore, 560013, India. E-mail: yelamaggad@gmail.com*

† Electronic supplementary information (ESI) available. See DOI: 10.1039/c4nj00426d

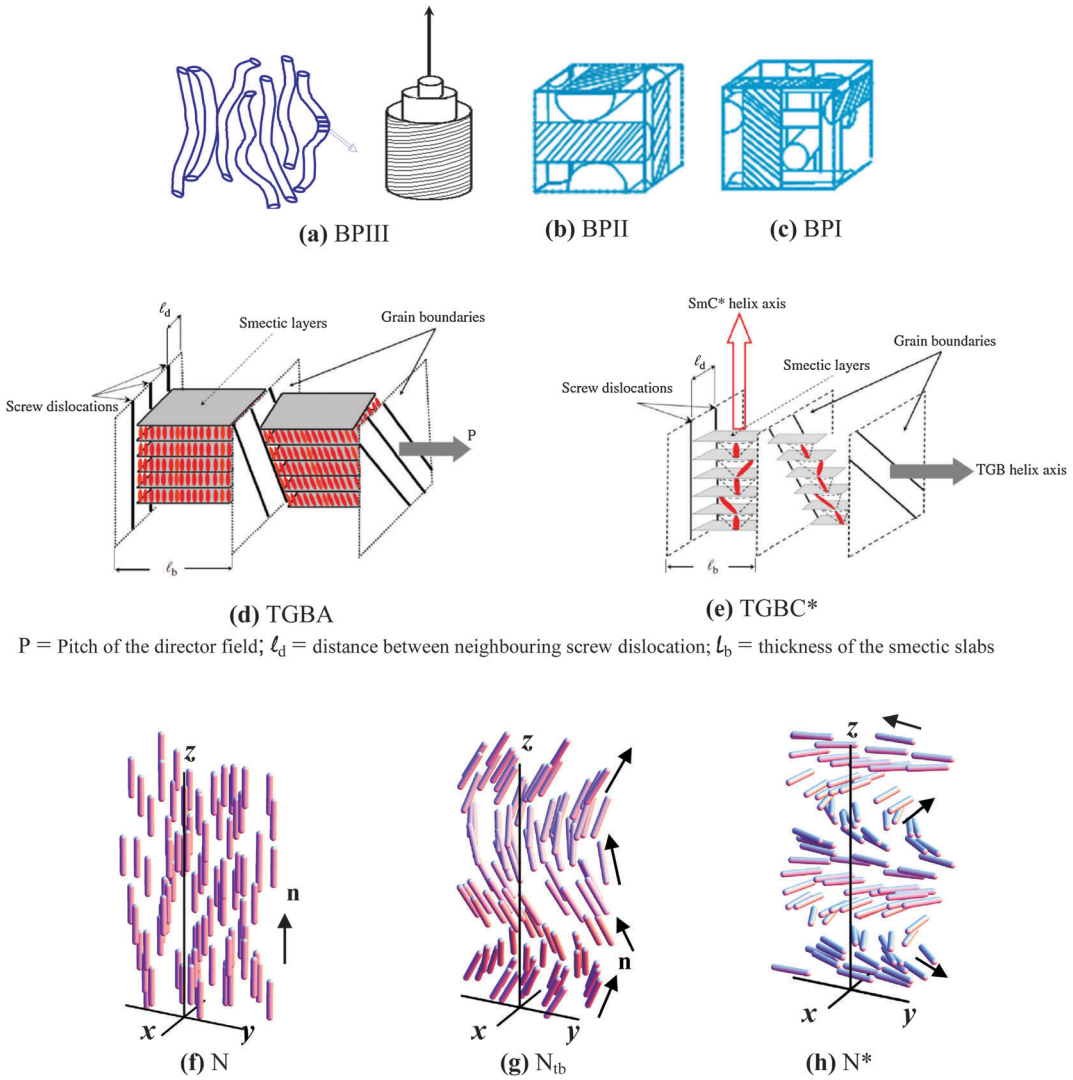

Fig. 1 Schematic illustration of the molecular arrangement in the frustrated phases (a) the spaghetti model representation of a BPIII phase (left portion) having randomly oriented squirming double twist tubes (right portion). Spatial arrangement of the double twist cylinders in (b) the simple cubic structure of BPII and (c) the body centred cubic structure of BPI. (d) TGBA and (e) TGBC* phases. Disposition of the molecules in (f) the N phase where the director, **n**, is globally uniform, (g) the N_{tb} phase with the local director following oblique helicoids and (h) the N* phase wherein the local director is normal to the helical axis, *z*. (d) and (e) are reprinted with permission from ref. 15*k*; (f–h) are reprinted with permission from ref. 8.

LC dimers.[6j] Thus, symmetric dimers are turning out to be interesting materials.

Likewise, non-symmetric dimers, especially the chiral systems formed by tethering pro-mesogenic cholesterol to one of the termini of a rod-like mesogen *via* a flexible spacer of varying length and parity, exhibit significant phase transition properties.[10] For example, different types of frustrated structures, re-entrant phenomena and unprecedented sequences have been observed in these materials. They show the critical dependence of transition temperatures and enthalpies on the parity of the central flexible spacer. Their behaviour is also governed by the relative lengths of the spacer and terminal tail as well as the chemical nature of the rod-like (non-cholesteryl) mesogen attached to cholesterol. It is shown that using appropriate combinations of these chemical parameters one can modulate the physical properties of technologically important LC phases.[10] Although the LC behaviour of a large number of cholesterol-based dimers belonging to different series has been accumulated, a complete understanding of the structure–property correlation is still difficult as subtle modifications to the molecular structure bring about a drastic change in the LC properties.[10]

These observations prompted us to design and synthesize cholesterol-based non-symmetric dimers with variation in the molecular structure of aromatic mesogenic unit and the length (and parity) of the central spacer. For example, there have been some interesting reports on such dimers where the significance of non-chiral aromatic segments such as Schiff's base, salicylaldimine, azobenzene, stilbene, tolan, biphenyl, sydnone, chalcone, oxadiazole or cinnamate units has been well demonstrated.[11–15] Among these, the chalcone unit, where two phenyl rings are interconnected through an α,β-unsaturated carbonyl group, being a small bent-core unit, has been found to

enhance the chirality of the dimers when connected to cholesterol through a spacer.[15h,i] From the point of view of material sciences, they have gained prominence as non-linear optically active (NLO) materials with excellent blue-light transmittance and good crystallizability.[16] With two planar rings connected through a conjugated double bond, they provide the necessary configuration to display NLO properties. 4,4′-Difluorochalcone is especially used in the synthesis of NLO active polymers.[17] Prompted by these observations and in continuation of our quest to synthesize novel dimeric materials we chose to incorporate chalcone as the non-cholesteryl mesogen in a cholesterol-based dimeric structure. In view of the fact that the majority of the dimers realized earlier by our group derived from chalcone–cholesterol combinations (see Chart 1, **4DC-*n,m*** series) exhibit frustrated phases over a wide thermal range,[15h,i] we were inspired to undertake a systematic investigation on analogous dimers to possibly understand the correlation between molecular structure and thermal properties. As possible modifications to the parent series, we prepared as many as four (1 to 4) series of dimers; the general molecular structures of the four series of dimers are shown in Chart 1. While the length of the terminal tail was varied in the first series, the length and parity of the central ω-oxyalkanoyl spacer were varied commonly in all series of dimers.

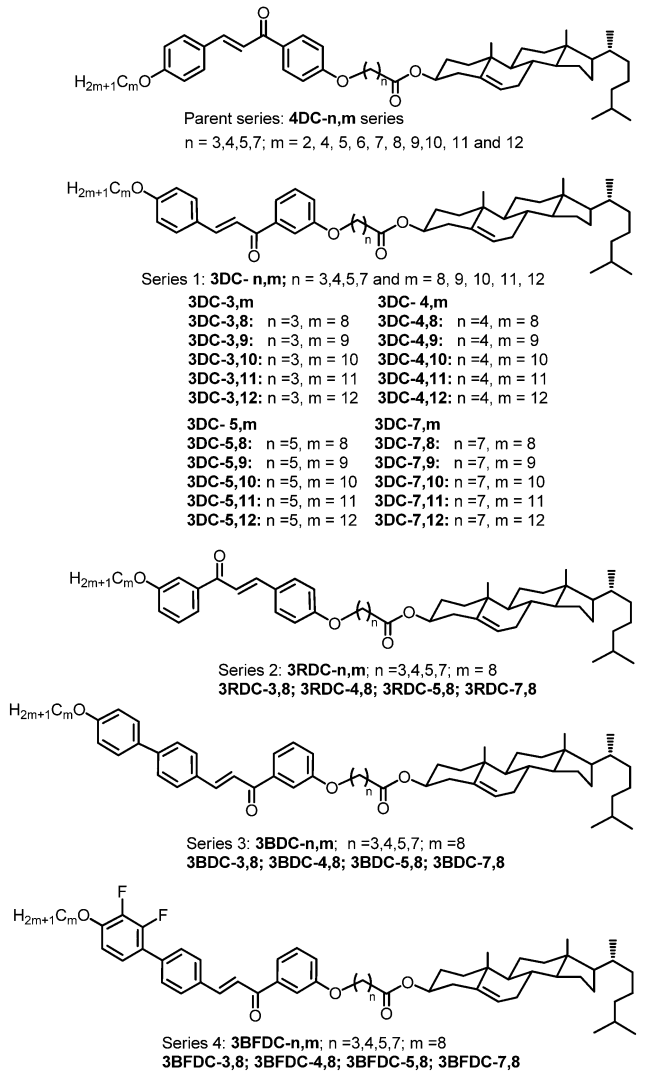

Chart 1 Molecular structures of cholesterol-based dimers belonging to previous (**4DC-*n,m*** series) and present (series **1–4**) studies.

At the start, we altered the position of attachment of the spacer to the mesogenic (non-cholesteryl) segment; that is, a homologous series of dimers were prepared (series 1: **3DC-*n,m***) by *o*-alkylating 4-*n*-alkoxy-3′-hydroxy chalcones with cholesteryl ω-bromoalkanoates. Given the fact that the α,β-unsaturated carbonyl group of the chalcone unit is polar, we reversed the position of such a group which may invert the direction of the polarity of the dimers. This alteration resulted in dimers of series 2 (**3RDC-*n*** series) where the substitution of the terminal chain is at the 3-position with respect to the carbonyl moiety attached to the terminal phenyl ring. The increase in the length of the aromatic (phenyl) ring by attaching another phenyl ring promotes the lateral interactions and to visualize its effect on the thermal behaviour we have synthesized another series (series 3: **3BDC-*n***) where the long chalcone core (having a biphenyl ring) is joined to cholesterol through a spacer of varying length and parity. Owing to its small size and high electronegativity, the fluorine atom has long been used to generate lateral dipoles, minimize viscosity, and lower transition temperatures as well as to alter the phase transition behaviour of LCs.[18,19] Keeping these points in view, we created another series of dimers (series 4: **3BFDC-*n***) where the lateral fluoro substituted, long-chalcone core is tethered to cholesterol *via* a spacer. Thus, in the four series of dimers realized, two primary structural modifications with respect to the parent series were incorporated: (i) altering the relative positions of the cholesteryloxycarbonyl-*n*-alkane and/or *n*-alkoxy tail attached to each of the two phenyl rings of chalcone (series 1 and 2) and (ii) elongating one of the aryl rings with or without lateral fluoro substitutions of chalcone ring (series 3 and 4).

II. Results and discussion

II.1. Synthesis and molecular structural characterization

The synthetic route adopted to prepare the target dimers and their precursors is outlined in Scheme 1. Cholesteryl ω-bromoalkanoates (**1a–d**) were synthesized by treating cholesterol with the freshly prepared 4-bromobutanoyl, 5-bromopentanoyl, 6-bromohexanoyl or 8-bromooctanoyl chlorides, as reported in the literature.[20,21] The key intermediates, namely hydroxy chalcones **3a–e**, **6**, **9** and **13**, were prepared as described in the literature[22] wherein various alkylaryl ketones were condensed with appropriate aldehydes in the presence of a methanolic solution of KOH, which we briefly describe as follows. The requisite 4-(*n*-alkoxy)benzaldehydes **2a–e** were prepared by the *O*-alkylation of 4-hydroxybenzaldehyde with the appropriate *n*-bromoalkane in butanone using anhydrous K_2CO_3 as a mild base. These 4-*n*-alkoxybenzaldehydes (**2a–e**) were condensed with 3-hydroxyacetophenone to yield (*E*)-1-(3-hydroxyphenyl)-3-(4-*n*-alkoxyphenyl)prop-2-en-1-ones (**3a–e**). Compound **6**,

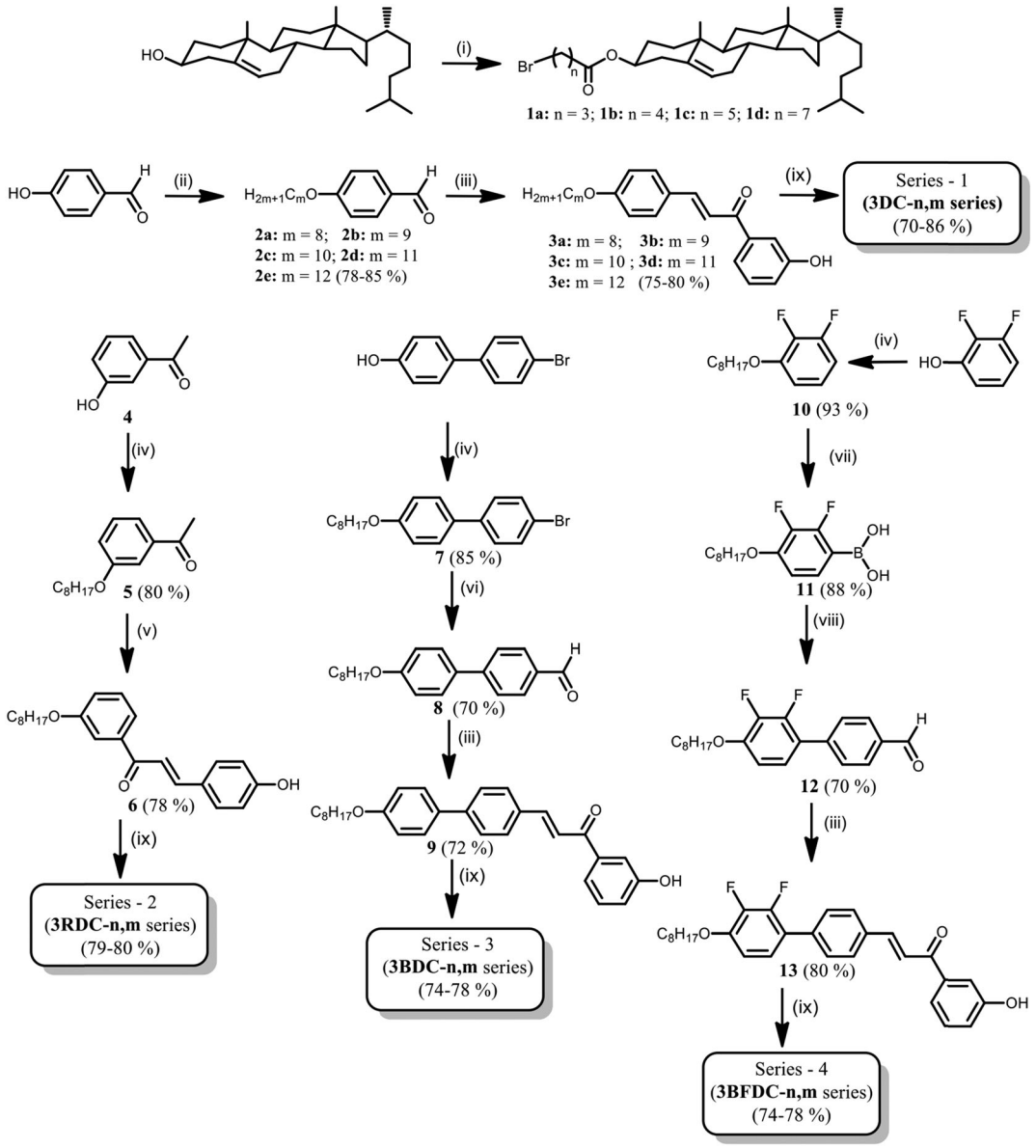

Scheme 1 Synthesis of four series of cholesterol-based dimers. Reagents and conditions: (i) *n*-bromoalkanoyl chlorides, pyridine, THF, 0–5 °C to rt, 8 h; (ii) *n*-bromoalkane, anhydrous K_2CO_3, butanone, reflux, N_2, 12 h; (iii) 3-hydroxyacetophenone, KOH, methanol, reflux, 12 h; (iv) 1-bromooctane, anhydrous K_2CO_3, butanone, 80 °C, 12 h; (v) 4-hydroxybenzaldehyde, KOH, methanol, 60 °C, 12 h; (vi) *n*-BuLi, DMF, THF, N_2, −78 °C to rt, 12 h; (vii) (a) *n*-BuLi, triisopropyl borate, THF, N_2, −78 °C to rt, 12 h; (b) 10% HCl (aq); (viii) 4-bromobenzaldehyde, 2 M Na_2CO_3 (aq) solution, $Pd(PPh_3)_4$, benzene, ethanol, reflux; (ix) **1a–d**, anhydrous K_2CO_3, DMF, N_2, 80 °C, 12 h.

(*E*)-3-(4-hydroxyphenyl)-1-(3-(octyloxy)phenyl)prop-2-en-1-one, was prepared starting from 3-hydroxyacetophenone, which was first *O*-alkylated with *n*-octyl bromide in the presence of anhydrous K_2CO_3 in butanone, followed by condensation of **5** with 4-hydroxybenzaldehyde. Subsequently, chalcone **9**, (*E*)-1-(3-hydroxyphenyl)-3-(4′-(*n*-octyloxy)biphenyl-4-yl)prop-2-en-1-one, was synthesized by reacting 4′-(*n*-octyloxy)biphenyl-4-carbaldehyde (**8**) with 3-hydroxyacetophenone. In turn, aldehyde **8** was prepared starting from 4′-bromobiphenyl-4-ol; it was *O*-alkylated with *n*-octylbromide in the presence of anhydrous K_2CO_3 to obtain 4-bromo-4′-(*n*-octyloxy)biphenyl (**7**); this was lithiated using *n*-butyllithium (*n*-BuLi) and thus, the *in situ* generated aryllithium reagent was quenched with dry DMF to obtain 4-*n*-octyloxy-4′-biphenyl aldehyde (**8**) in 62% yield. Next, the fluoro analogue **13**, (*E*)-3-(2′,3′-difluoro-4′-(*n*-octyloxy)biphenyl-4-yl)-1-(3-hydroxyphenyl)prop-2-en-1-one, of chalcone **9** was prepared in four steps as depicted in the scheme. 2,3-Difluorophenol was *O*-alkylated with *n*-bromooctane to get 1,2-difluoro-3-(*n*-octyloxy)benzene (**10**) in reasonably good yield. The aryllithium reagent generated by the reaction of compound **10** with *n*-BuLi in dry THF was treated with triisopropyl borate and borate ester thus obtained was subjected to hydrolysis using 10% HCl (aqueous) to give 2,3-difluoro-4-(*n*-octyloxy)phenylboronic acid **11**. Palladium catalysed Suzuki cross-coupling reaction of arylboronic

acid **11** with 4-bromobenzaldehyde furnished 2′,3′-difluoro-4′-(*n*-octyloxy)biphenyl-4-carbaldehyde (**12**), which upon treating with 3-hydroxy acetophenone under basic reaction conditions yielded chalcone **13**. Finally, the target dimers were prepared by *O*-alkylation of hydroxy chalcones **3a–e**, **6**, **9** and **13** with appropriate cholesteryl ω-bromoalkanoates (**1a–d**) under typical Williamson ether synthesis conditions. The structures of all the intermediates and target molecules were confirmed using spectroscopic data and/or elemental analyses (see the ESI† for the details).

II.2. Thermal behavior

The mesomorphism of these new LC dimers belonging to four different series was investigated by polarizing optical microscopy (POM), differential scanning calorimetry (DSC) and X-ray diffraction (XRD). The occurrence of thermotropic LC phase(s) was initially verified based on the observation of strong birefringence and fluidity under POM. Explicit LC phase assignment was made according to the characteristic textural pattern seen. The peak temperatures obtained in the DSC traces due to phase transitions were found to be consistent with those of the POM studies. The transition temperatures and the corresponding enthalpies derived from DSC traces of the first heating–cooling cycles at a rate of 5 °C min^{-1} are given. In the following sections, we present the details of the LC behaviour of the dimers derived from the studies using the above-mentioned complementary techniques.

II.2.1. Series 1 (3DC-*n*,*m* series). As can be seen in Chart 1, in this series, the cholesterol is covalently linked to chalcone through either trimethylene (*n* = 3; 4-oxybutanoyl; even-parity) or tetramethylene (*n* = 4; 5-oxypentanoyl; odd-parity) or pentamethylene (*n* = 5; 6-oxyhexanoyl; even-parity) or heptamethylene (*n* = 7; 8-oxyoctanoyl, even-parity) spacers; while the chalcone is substituted with *n*-octyloxy to *n*-dodecyloxy (*m* = 8 to 12) tails. These structural variations give rise to four sub-homologous (**3DC-3,*m***, **3DC-4,*m***, **3DC-5,*m*** and **3DC-7,*m***) series of dimers. Thus, the thermal behavior (transition temperatures and enthalpies) of **3DC-3,*m***, **3DC-4,*m***, **3DC-5,*m*** and **3DC-7,*m*** series of dimers comprising 4-oxybutanoyl, 5-oxypentanoyl, 6-oxyhexanoyl, and 8-oxyoctanoyl spacer is summarized in Table 1.

As can be seen, the dimers of **3DC-3,*m*** having 4-oxybutanoyl (even-parity) spacer exhibit chiral nematic (N*) phases only. In particular, the N* phase is enantiotropic for the first dimer **3DC-3,8**, while it is monotropic in higher members. Seemingly, this trend is in contrast to the general observation that in a given homologous series of low molar mass (monomeric) LCs the mesophases are often metastable for lower members, and only the higher homologues display enantiotropic behavior;[1c,d] the monotropic phase transitions of the lower homologues can be accounted for by their higher melting temperatures as the cause of the reduced flexibility. The N* phase was identified by optical textural observation. When examined under POM in the form of a thin film of sample prepared between two untreated glass slides and cooled from the isotropic phase (I), the focal-conic texture was obtained, which on mechanical stressing yielded an oily streak pattern. The focal-conic and oily streak textures, as shown in shown in Fig. 2a and b respectively, for dimer **3DC-3,8** as a representative case, are typical of the N* phase. Compared to the occurrence of smectic A (SmA) and/or N* phase(s) in dimers with an identical spacer of the parent **4DC-*n*,*m*** series, these compounds exhibit only the N* phase, which points to the importance of the position at which the

Table 1 Transition temperatures (°C)[a] and enthalpies (J g^{-1}) of **3DC-*n*,*m*** series of dimers[f]

	Phase sequence	
Dimer **3DC-3,*m***	Heating	Cooling
3DC-3,8	Cr 115.4[b] [16.5] N* 121.7 [3] I	I 120.7 [3] N* 93.4 [32.5] Cr
3DC-3,9	Cr 128.6 [62.9] I	I 120.7 [3.3] N* 100.9 [42.8] Cr
3DC-3,10	Cr 133.3 [63.8] I	I 118.9 [3.4] N* 107.5 [42.2] Cr
3DC-3,11	Cr 135.6 [57.5] I	I 116.2 [3.1] N* 111.9 [48.5] Cr
3DC-3,12	Cr 132.8 [62.8] I	I 118.2 [3.9] N* 111.6 [47.6] Cr
3DC-4,8	Cr 130.8 [82] I	I 80.5 [56.2] Cr
3DC-4,9	Cr 105.5 [63.9] I	I 78.4 [49.5] Cr
3DC-4,10	Cr 101.4[c] [49.8] I	I 82.4 [42.4] Cr
3DC-4,11	Cr 107.3 [62.7] I	I 89.7 [58.3] Cr
3DC-4,12	Cr 118.5 [79.6] I	I 93.8 [55.5] Cr
3DC-5,8	Cr 97.9 [55.7] N* 110.8 [3.6] I	I 109.8 [3.5] N* 71.9[d] TGB 57[d] Cr
3DC-5,9	Cr 98 [55.2] N* 109.9 [3.8] I	I 108.9 [3.7] N* 82.8[d] TGB 64[d] Cr
3DC-5,10	Cr 99.9 [47] N* 109.2 [3.9] I	I 108.2 [3.8] N* 48.7 [14.9] Cr
3DC-5,11	Cr 105.8 [47.8] N* 108.1 [3.5] I	I 107.2 [3.4] N* 86.4[d] TGBC* 68.2 [30.1] Cr
3DC-5,12	Cr 109.1[e] [25.8] I	I 106.4 [4.3] N* 76.6 [0.5] TGBC* 72.6 [31.9] Cr
3DC-7,8	Cr 86.2 [59.5] N* 104.8 [4.4] I	I 104.1 [4.2] N* 84.8[d] TGB 74[d] SmA 42.2 [5] Cr
3DC-7,9	Cr 85.6 [62.5] N* 104.1 [4.6] I	I 102.9 [4.4] N* 78.6[d] TGB 65.3[d] SmA 43[d] Cr
3DC-7,10	Cr 89.9 [64.2] N* 102.8 [4.3] I	I 101.9 [4.5] N* 77.3[d] TGB 72.3[d] SmA 39[d] Cr
3DC-7,11	Cr 88.8 [64.2] N* 102.2 [4.5] I	I 101.5 [4.4] N* 73.6[d] TGB 46[d] Cr
3DC-7,12	Cr 94.7 [62.6] N* 104.4 [4.6] I	I 103.9 [4.7] N* 80.5[d] TGBC* 61.1 [11.1] Cr

[a] Peak temperatures in the DSC thermograms obtained during the first heating and cooling cycles at 5 °C min^{-1}. [b] A crystal to crystal transition was observed at 113.5 °C [10.7 J g^{-1}]. [c] A crystal to crystal transition was seen at 96 °C [19.4 J g^{-1}]. [d] The phase transition observed under POM was too weak to be detected by DSC. [e] Crystal to crystal transitions were observed at 75.1 °C [5 J g^{-1}] and 103.8 °C [37.3 J g^{-1}]. [f] Cr = crystal; N* = chiral nematic phase; TGB = twist grain boundary phase with smectic A (SmA)/smectic C (SmC) slabs; TGBC* = twist grain boundary phase with SmC* slabs. I = isotropic liquid state (these abbreviations are applicable wherever mentioned).

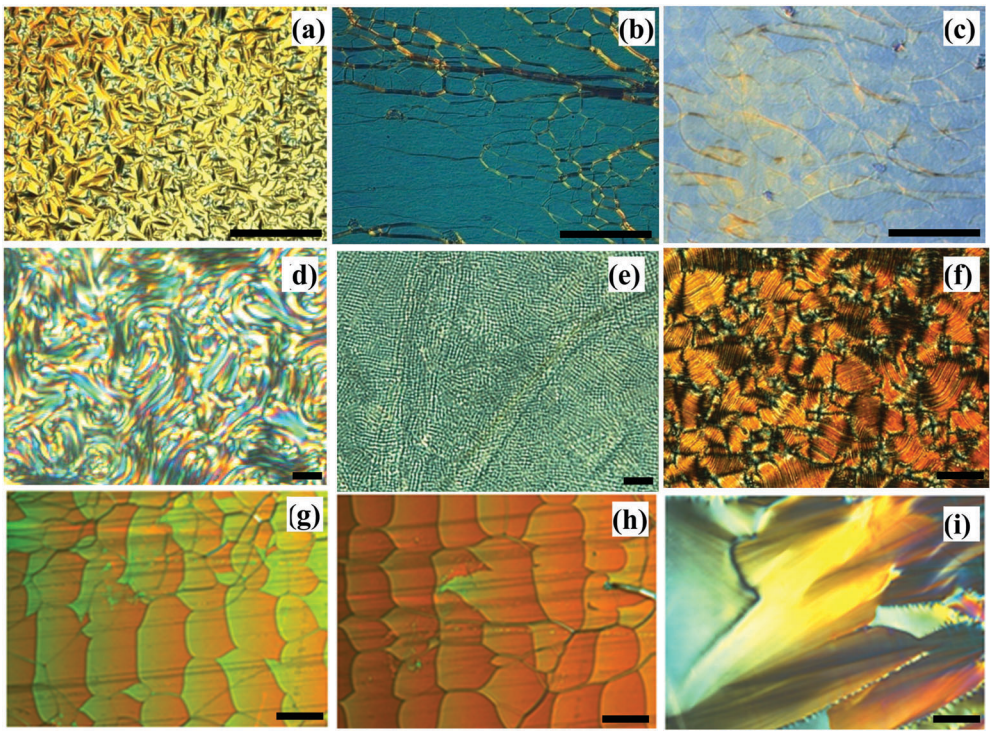

Fig. 2 Photomicrographs of optical textures seen under POM for the LC phases of dimers of series-1 (**3DC-*n*,*m*** series): (a) focal-conic texture of the N* phase seen at 117 °C while cooling **3DC-3,8** from the isotropic phase; (b) oily streak texture obtained upon shearing the focal-conic pattern of the N* phase (at 117 °C) of **3DC-3,8**; (c) planar texture of the TGB phase formed at 71 °C on cooling the planar aligned N* phase of **3DC-5,9**; (d) filamentary texture seen for the TGB phase at 65 °C for the homeotropically aligned **3DC-5,9**; (e) square grid pattern of the TGBC* phase seen for dimer **3DC-5,11** at 92 °C; (f) texture of the TGBC* phase grown at 72 °C on top of the focal-conic pattern of the N* phase of **3DC-5,11**; (g) GC dislocation lines observed at 87 °C for the N* phase of **3DC-7,8**; (h) GC dislocation lines noticed at 82 °C for the TGB phase of **3DC-7,8**; (i) focal-conic texture of the SmA phase existing just below the TGB phase (74 °C). (Bar: 100 μm).

cholesteryloxycarbonyl-*n*-alkane is attached to the chalcone in determining the phase behaviour. It may be noted here that the **3DC-3,*m*** series of compounds display lower N*–I or Cr–I transition temperatures than those of the analogous parent dimers, implying the possibility of the **3DC-3,*m*** series of molecules attaining bent conformations.

Contrary to expectation, none of the dimers belonging to **3DC-4,*m*** series exhibits mesomorphic behaviour (see Table 1) despite possessing a pro-mesogenic cholesterol segment. However, the loss of mesomorphism in these dimers can be duly interpreted in terms of their pronounced bent molecular conformation and thus reduced shape anisotropy. Specifically, in these dimers the cholesterol and 4-*n*-alkoxychalcone anisometric segments are inclined with respect to each other as they are linked by an odd-parity (5-oxypentanoyl; C_5) spacer. Thus, the overall molecular shape considered in the all-*trans* conformation of these dimers (Fig. 3a) is bent as against the linear shape of the **3DC-3,*m*** series of dimers wherein the two mesogenic segments are separated by an even-parity spacer (Fig. 3b). It is important to remark here that when compared to the noteworthy thermal behaviour of the parent series of compounds[15h,i] having a 5-oxypentanoyl spacer, especially the dimers with *n*-decyloxy to *n*-dodecyloxy (m = 10 to 12) tails,[15h] the **3DC-4,*m*** series of dimers fail to exhibit LC properties.

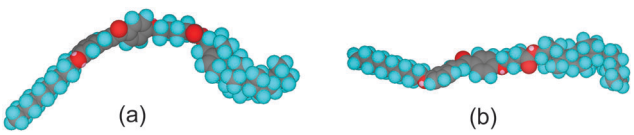

Fig. 3 Energy minimized structures of dimers (a) **3DC-4,10** and (b) **3DC-3,10**. Note that mesogenic segments of the dimer **3DC-4,10** with an odd-parity spacer are inclined with respect to each other.

It can be seen from Table 1 that the dimers of the **3DC-5,*m*** series, wherein the cholesterol and chalcone cores are separated by a 6-oxyhexanoyl (even-parity) spacer, show LC behaviour. The first two compounds *viz.*, **3DC-5,8** and **3DC-5,9** of the series exhibit an enantiotropic N* phase in addition to a monotropic TGB phase. The existence of the N* phase was ascertained based on textural observation; for example, when a thin film of the isotropic liquid of dimer **3DC-5,9**, contained in either normal glass plates or substrates treated for planar alignment, was cooled slowly, a focal-conic texture was observed, which on mechanical shear changes to a planar pattern. On further cooling, the Grandjean planar texture of the N* phase transforms sharply to yet another but distinct deep gray blurry planar texture as shown in Fig. 2c. Such a planar pattern is reported to be seen for the TGB phase[23–25] in which the molecular long axes are parallel to the substrate and thus the

smectic (SmA or SmC) layer planes are perpendicular to the glass plates. On cooling the sample further, the planar texture gradually converts to a blurred focal-conic texture. When the sample was subjected to homeotropic boundary conditions to attain the long molecular axis orientation perpendicular to the substrates, the N* and TGB phases showed the focal-conic and vague vermis (filamentary) (Fig. 2d) patterns respectively.[24a] All these optical observations clearly indicate that these two dimers exhibit a dimesomorphic sequence involving a transition from the N* to the TGB phase. The occurrence of a TGB phase over a 15 °C thermal range is noteworthy in light of the fact that such phases, being frustrated, are known to exist only for short thermal range,[4] except for a few cases.[15h,i]

The next dimer **3DC-5,10** exhibits an enantiotropic N* phase exclusively over a wide thermal range (about 60 °C) indicating that a slight variation (lengthening) of the terminal tail greatly influences the phase behaviour of these dimers. Based on the behaviour of dimer **3DC-5,10** it may be reasonable to presume that the higher members of this compound would continue to show the N* phase. In contrast to this assumption, the next higher homologue **3DC-5,11** exhibit a monotropic TGBC* phase besides the enantiotropic N* phase. Surprisingly, these two phases were found to be metastable for the next higher dimer **3DC-5,12**. The occurrence of a dimesomorphic sequence was adjudged based on the textural observation, which we briefly discuss for the dimer **3DC-5,11**. This dimer exhibits an N* phase with a planar texture in which the nematic director lies in the plane of the substrate. This ensures that the helical axis is perpendicular to the glass plates *i.e.*, along the viewing direction. On further cooling, the transition to another phase was noticed wherein the planar texture of the N* phase sharply changes to a square grid pattern as shown in Fig. 2e, which is reported to be an important signature for the existence of a complex and highly frustrated mesophase, namely the twist grain boundary (TGB) phase possessing chiral smectic C (SmC*) blocks, denoted as the TGBC*[15i–l,25–28] According to Galerne's model of the TGBC* phase,[25] in addition to the tilt of the molecules with respect to the smectic layer normal, there is a precision of the SmC director, resulting in a second helix orthogonal to the TGB helix axis; consequently, each smectic block has a smectic C* structure (Fig. 1e, right). A direct consequence of this is the appearance of the square grid pattern. Experimentally, it has been observed that the TGBC* phase indeed exhibits a square grid pattern superimposed on the planar texture as mentioned above. When the sample was examined in slides treated for homeotropic alignment and cooled from the focal-conic texture of the N* phase, a non-specific texture consisting of some tiny undulated filaments was seen as shown in Fig. 2f. The occurrence of a tiny grid pattern or indistinct undulated filaments perhaps implies that pitch of the helix is short. In comparison, the thermal behavior of the **3DC-5,*m*** series of dimers having a 6-oxyhexanoyl (even-parity) spacer is markedly different from the analogous parent dimers. As discussed above, except for dimer **3DC-5,12**, all the compounds display an enantiotropic mesophase; whereas the corresponding dimers of the parent series display metastable mesophases with the exception of the compound having an *n*-dodecyloxy tail. Interestingly, the dimer **3DC-5,12** displays two monotropic mesophases featuring helical structures while the analogous dimer of the parent series stabilizes an enantiotropic layered mesophase, the SmA phase. It can be therefore inferred that these dimers have reduced shape anisotropy owing to their bent molecular shapes.

All the dimers with an 8-oxyoctanoyl (even-parity) spacer of the **3DC-7,*m*** series display an enantiotropic N* phase in addition to one or two monotropic phases such as TGB, SmA and TGBC* as summarized in Table 1. The first three dimers *viz.*, **3DC-7,8**, **3DC-7,9** and **3DC-7,10** exhibit an enantiotropic N* phase as well as monotropic TGB and SmA phases which was ascertained by optical textural observation. When a thin film of these dimers placed between a slide and a cover slip was cooled slowly from the isotropic phase, the transition to the N* phase occurs with the characteristic focal-conic texture that on mechanical shear changes to a planar pattern. Upon cooling the sample further from the Grandjean planar (oily streak) texture of the N* phase, a transition to another mesophase takes place with a gray blurry planar texture, which is typical of the TGB phase. On further cooling, a phase transition was noticed with a textural pattern consisting of blurred focal-conic fans accompanied by some planar regions of the TGB phase. On lowering the temperature further, in some regions of the slide, especially at the edges, well-defined focal-conic fans typical of an SmA phase were noticed. When these samples were examined between glass slides treated for homeotropic alignment, the N* and TGB phases respectively showed focal-conic and vague vermis (filamentary) patterns.[24a] In order to elucidate the phase sequence further, the dimer **3DC-7,8** as a representative case was investigated in a wedge type cell treated for planar orientation wherein the thickness varies from one end to other. On cooling the isotropic liquid, Grandjean Cano (GC) dislocation lines (striations running from the top to bottom of the pattern) were observed for the N* and TGB phases, as shown in Fig. 2g and h respectively, demonstrating that there is a helical twist normal to the plates in these phases.[15h–i,26] On cooling the sample further from the planar texture having GC dislocation lines of the TGB phase, these dislocation lines become progressively wider, and disappear leaving behind only the planar pattern. Nearing the transition to the SmA phase, the TGB phase exhibits a texture wherein the fine arcs over the planar pattern move randomly and rapidly. When the transition to the SmA phase takes place, this planar pattern transforms sharply into a texture consisting of focal-conic fans as shown in Fig. 2i. Thus, these experimental results ascertain the existence of N*, TGB (with either SmA or SmC slabs) and SmA phases in these dimers. As shown in Table 1, the dimers **3DC-7,11** and **3DC-7,12** with relatively longer terminal tails exhibit a dimesomorphic sequence involving a transition from N* to TGB and N* to TGBC* phases, respectively. It is worth mentioning here that the above-mentioned phase sequences of these dimers, including the other series of materials, are highly reproducible which clearly demonstrates their thermal stability.

Within the series, the melting and clearing temperatures of these dimers seem not to vary much as a function of terminal tail length; however, upon ascending the series, the smectic behaviour is extinguished with exclusive occurrence of a TGB phase. A general comparison of the phase behaviour of these dimers belonging to the **3DC-7,*m*** series with those of the analogous parent systems shows that they commonly exhibit N* and frustrated phases with optional SmA phases; remarkably, the former dimers show a TGB phase below the N* phase while the latter ones display BP above the N* phase. The melting and clearing temperatures of the present series of dimers are at least 20 °C below the analogous parent systems indicating that the former systems are perhaps twisted to some extent.

It is now well documented that the structure (periodicity) of the SmA phase formed by cholesterol-based dimers decisively depends upon the relative lengths of the spacer and terminal chains.[10a,11–15,29] Thus, the SmA phase of dimer **3DC-7,8**, in which the length of the terminal tail and spacer are equal, was investigated by powder X-ray diffraction (XRD), as a representative case. The results of indexing of the XRD profile are summarized in Table 2. The diffractogram obtained at 70 °C showed a sharp peak in the low angle region with a *d*-value of 24.7 Å that can be attributed to originating from the layered structure. In addition, a typical diffuse scattering in the wide angle region (d = 4.9 Å) was observed pointing to a liquid like order within the smectic layers. The calculated length of the molecule (l) using a Chem3D molecular model is 50.61 Å. Thus the d/l ratio is 0.49, which points to the formation of an intercalated SmA phase as shown in Fig. 4. It can therefore be inferred that cholesterol-based dimers stabilize an intercalated SmA phase if they possess terminal tails and flexible spacers of equal length.

Thus, among the four sub series of dimers synthesized, all the five compounds of **3DC-4,*m*** series having odd-parity spacers are non-mesomorphic, while the other three homologous series of compounds *viz.*, **3DC-3,*m***, **3DC-5,*m*** and **3DC-7,*m*** formed by varying the length of the even-parity spacer are liquid crystalline. It is quite apparent from the comparison of the thermal behaviour of these three series of dimers that the nature and extent of mesomorphism are dependent on the length of the even-parity spacer. For example, all the homologues

Table 2 The results of indexing of XRD profiles of dimers at a given temperature (T) of mesophases; the estimated all-*trans* molecular length (l); layer spacings (d/Å); d/l ratio and structural assignment of the smectic phases of dimers. SmC*: chiral smectic C phase

Dimer	T (°C)	d (Å)	l (Å)	d/l	Nature of the phase
3DC-7,8	70	24.7 4.9	51	0.48	Intercalated SmA
3RDC-3,8	122	45.1 22.3 5.1	47	0.96	Monolayered SmA
	60	43.8 5	47		SmC* (tilt angle 21.6°)
3BDC-7,8	145	26.3 5.1	54	0.49	Intercalated SmA
3FDC-7,8	100	25.2 5	53	0.48	Intercalated SmA

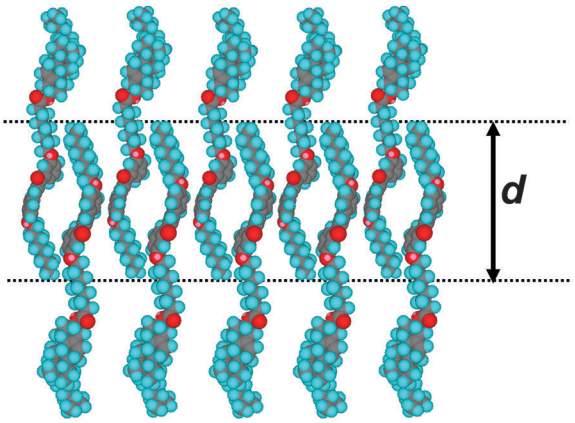

Fig. 4 A schematic representation of the self-assembly of dimer **3DC-7,8** into an intercalated SmA phase. Notice that the terminal alkyl chains and the spacers are mixed.

of the **3DC-3,*m*** series exhibit an N* phase and the thermal range of this phase decreases with an increase in the length of the terminal chain. In the **3DC-5,*m*** series, except for the dimer with an *n*-decyloxy tail which exhibits only the N* phase, all the compounds stabilize frustrated mesophases like TGB or TGBC* besides the N* phase; interestingly, alternation of the N*-TGB or N*-TGBC* transition temperature as a function of the number of carbon atoms in the terminal chain occurs. Within the **3DC-7,*m*** series of dimers, the length of the terminal tail influences the phase behaviour; the dimers with *n*-octyloxy to *n*-decyloxy tails stabilize a trimesomorphic sequence *viz.*, N*-TGB–SmA, while compounds comprising *n*-undecyloxy and *n*-dodecyloxy chains display a dimesomorphic sequence involving a transition from N* to TGB/TGBC* phase; here also a marginal transition temperature alternation as a function of the length of the terminal chain persists. A common feature of these three sets of compounds is that within each series the isotropic liquid to mesophase transition temperature remains more or less the same regardless of the terminal chain length. It may also be noted here that the LC to isotropic liquid phase transition temperature reduces progressively upon lengthening the spacer. Contrary to the occurrence of a blue phase in the vast majority of the dimers of the parent series, none of these dimers displays such a frustrated structure. Therefore, in comparison to the parent series, these dimers showed different thermal behaviour, thus signifying the fact that even a small variation in the molecular structure will lead to a dramatic change in the mesomorphic behavior of chiral dimers. This clearly indicates that the stabilization of the frustrated phases involves a delicate balance between the length, parity, and position of attachment of the spacer, structure of the aromatic mesogenic unit and the length of the terminal chain.

II.2.2. Series 2 (3RDC-*n*,*m* series). In this series of dimers, as compared to materials belonging to the **3DC-*n*,*m*** series, the positions of the *n*-alkoxy tail and cholesteryloxycarbonyl-*n*-alkane substituents of chalcone are interchanged. In other words, the chalcone linkage is reversed which perhaps imparts a different (linear) conformation to the molecule when compared to the members of the **3DC-*n*,*m*** series. Thus, it would be

Table 3 Transition temperatures (°C)[a] and enthalpies (J g^{-1}) of **3RDC-*n*,*m*** series[e]

Dimer **3RDC-*n*,8**	Phase sequence	
	Heating	Cooling
3RDC-3,8	Cr 117.3 [42.2] SmA 135.3 [9.5] I	I 132.6 [9.4] SmA 64[b] SmC* 42[c] Cr
3RDC-4,8	Cr 107.1 [45.6] I	I 92.4 [42.8] Cr
3RDC-5,8	Cr 100.7 [38.9] SmA 114.4[b] TGB 118.4 [1.5] N* 122.5 [2.5] I	I 121.6 [2.4] N* 117.3 [1.3] TGB 113.6[b] SmA 66.1[b] SmC*[d]
3RDC-7,8	Cr 102.1 [1.1] N* 113.3 [3.7] I	I 112.2 [3.2] N* 100[b] TGB 88 [b]SmA 88.8 [46.3] Cr

[a] Peak temperatures in the DSC thermograms obtained during the first heating and cooling cycles at 5 °C min^{-1}. [b] The phase transition was observed under polarizing microscope and was too weak to be recognized by DSC. [c] The SmA–Cr phase transition observed with a microscope was too weak to be detected by DSC. [d] The mesophase freezes into glassy state instead of crystallization. [e] SmA = smectic A; SmC* = smectic C phase (applicable wherever mentioned).

interesting to compare the thermal behaviour of the **3RDC-*n*,*m*** series of dimers with that of the **3DC-*n*,*m*** series. Table 3 gives the transition temperatures and associated enthalpies of these four dimers belonging to the **3RDC-*n*,8** series. From the results it can be seen that the dimer **3RDC-4,8** having an odd-parity (5-oxypentanoyl) spacer is non-mesomorphic which can be ascribed to its pronounced bent conformation and thus, reduced shape anisotropy of the molecule; this is analogous to the behaviour of dimer **3DC-4,8**. On the other hand, dimers **3RDC-3,8**, **3RDC-5,8** and **3RDC-7,8** composed of even-parity spacers exhibit mesomorphic behavior, which we briefly describe as follows. When the dimer **3RDC-3,8** was placed between two glass slides treated for planar anchoring conditions and cooled slowly from the isotropic liquid, a striking focal-conic texture typical of the SmA phase was obtained. On cooling the sample further, dechiralization lines appeared on the top of the focal conic texture, characteristic of a SmC* phase. As expected, in slides treated for homeotropic orientation the SmA and SmC* phases displayed *pseudo*-isotropic and cloudy textures, respectively. It may be recalled here that **3DC-3,8**, the positional isomer of this dimer **3RDC-3,8**, displays an enantiotropic N* phase solely indicating that interchanging the relative positions of the *n*-alkoxy tail and cholesteryloxycarbonyl-*n*-alkane substituents of chalcone influences the phase behaviour significantly. The dimer **3RDC-5,8** displays enantiotropic N*, TGB and SmA phases besides a monotropic SmC* phase. This polymesomorphic sequence was established based on microscopic textural observation. Upon cooling the compound (taken between ordinary slides) from the isotropic phase, a focal conic texture appears for the N* which on shearing yielded a Grandjean planar texture; on cooling further (from the planar texture) a TGB phase appears with a planar textural pattern. On lowering the temperature further, a focal-conic texture, as shown in Fig. 5a, typical of the SmA phase was seen. When this phase was cooled further, a partially aligned focal-conic fan texture featuring dechiralization lines on top of it characteristic of the SmC* phase was observed (Fig. 5b). Upon lowering the temperature even further, the sample did not crystallize; instead the SmC* phase was found to be non-shearable at ~40 °C; this perhaps indicates the freezing of the SmC* phase into a glassy state. The DSC traces corroborated these observations where no peak was seen till −60 °C. In addition, the SmC* phase of this dimer was investigated for its ferroelectric switching characteristics by the method already described before. Surprisingly, contrary to our expectation, no electrical switching was observed. Even with quite large voltages, there was no sign of switching, and moreover, the sample could not sustain such high field strengths limiting further investigations. Thus, **3RDC-5,8** exhibits a polymesomorphic sequence *viz.*, N*–TGB–SmA–SmC*, while in comparison, the isomeric dimer **3DC-5,8** of the previous series shows a dimesomorphic (N*–TGB) sequence. Compound **3RDC-7,8** displays the N*–TGB–SmA phase sequence where the latter two phases were found to be monotropic in nature. Remarkably, the TGB phase exists for a thermal range of 18 degrees.

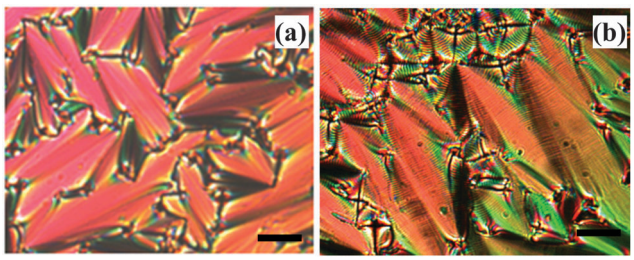

Fig. 5 Photomicrographs of the focal conic texture of the SmA phase (80.7 °C) (a) and focal conics with chiral lines obtained for SmC* phase (50 °C) of the dimer **3RDC-5,8** (b) (bar: 100 μm).

In order to provide more insight into the SmA and SmC* phases formed by dimer **3RDC-3,8**, XRD experiments were carried out. The X-ray intensity profiles obtained in the SmA phase at 122 °C and SmC* at 60 °C phase are presented in Fig. 6a and b respectively. The XRD data deduced from these profiles are summarized in Table 2. It can be seen that the low angle region of the diffractograms consists of two sharp reflections with *d*-values 45.1 Å and 22.3 Å for the SmA phase (Fig. 6a) and a sharp reflection at 43.8 Å for the SmC* phase (Fig. 6b). In addition, the diffractograms of SmA and SmC* phases show a diffuse peak in the wide angle region with *d*-values 5.1 Å and 5 Å respectively, which can be attributed to the intermolecular separation within the layer arising due to the liquid-like positional correlation of the flexible alkyl tails. The reflection at 22.3 Å seen for the SmA phase originates from some fragment of the dimers.[10a] The calculated length in the most extended form of the all-*trans* configuration of the molecule (*l*), measured using a Chem3D molecular model, is 47 Å. Hence the *d*-value 45.1 Å obtained for the SmA phase nearly corresponds to the length of the molecule (*l*), with a *d*/*l* ratio of 0.95 which is

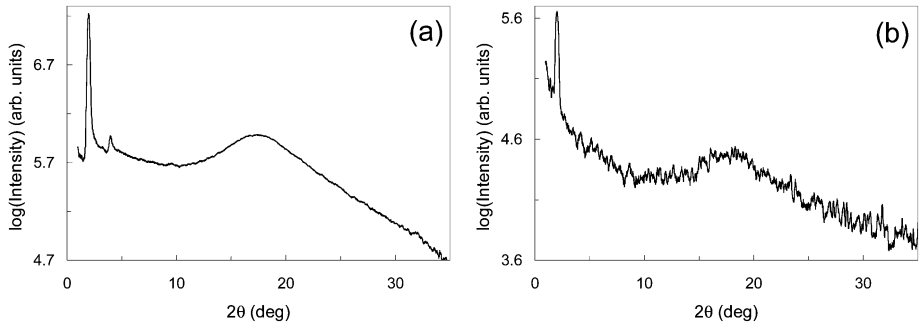

Fig. 6 The intensity *vs.* 2θ profiles extracted from the XRD patterns of the SmA phase at 122 °C (a) and SmC* phase at 60 °C (b) for the dimer **3RDC-3,8**.

characteristic of a monolayer SmA phase, whereas the layer spacing in SmC* with d = 43.8 Å, as expected, is less than the estimated all-*trans* molecular length, l = 47 Å, which indicates the tilted organization of the molecules within the smectic layers. The tilt angle, θ, of the molecules in this SmC* phase with respect to the layer normal was estimated to be ~21.6° using the expression $\theta = \cos^{-1}(d/l)$. In general, these dimers with chalcone linkages connected in a reverse fashion favour the formation of layered mesophases. Indeed, the length and parity of the spacer play an important role in dictating the mesophase behaviour of these dimers.

II.2.3. Series 3 (3BDC-*n*,*m* series). The phase sequences, transition temperatures and associated enthalpies of dimers of **3BDC-*n*,*m*** series are summarized in Table 4. It must be noted here that these four dimers are rather different from those of the parent series or the three series of compounds described above; they possess an elongated chalcone core where one of the phenyl rings is substituted by a biphenyl ring. Thus, the overall molecular length of these dimers is increased and consequently, as compared to the other three series of dimers described earlier, their clearing temperatures are higher. It is also important to mention here that the length and parity of the central spacer are varied while the terminal chain of the chalcone is kept constant with an *n*-octyloxy tail. The first member **3BDC-3,8** of the series having an 4-oxybutanoyl (even-parity) spacer exhibits enantiotropic N* and TGB phases besides a monotropic SmA phase. The striking filamentary texture seen while heating from a homeotropic aligned SmA phase is shown in Fig. 7a. When compared to the monomesomorphic (N*) and dimesomorphic (SmA–SmC*) behaviour of dimers **3DC-3,8** and **3RDC-3,8** respectively, this material stabilizes a trimesomorphic sequence, namely N*–TGB–SmA. Interestingly, the next dimer **3BDC-4,8** comprising an 5-oxypentanoyl (odd-parity) spacer, unlike the analogous dimer belonging to the **3DC-*n*,*m*** and **3RDC-*n*,*m*** series, displays mesomorphism; in particular, it shows the N* phase and BPs. On slow cooling the isotropic liquid, a mesophase appears at 154.7 °C with a bluish foggy texture of low birefringence

Table 4 Transition temperatures (°C)[a] and enthalpies (J g^{-1}) of **3BDC-*n*,8** series

	Phase sequence	
Dimer **3BDC-*n*,8**	Heating	Cooling
3BDC-3,8	Cr 138.7 [54] TGB 147.2[b] N* 183 [3] I	I 181.9 [2.8] N* 146.2[b] TGB 127[b] SmA 62[b] Cr
3BDC-4,8	Cr 135.3[c] [33.9] N* 157.2 [2.6] I	I 154.7 [1.1] BPIII[e] 152.7 BP 146.7 [1.1] N* 111.9 [27.3] Cr
3BDC-5,8	Cr 104.2 [29.7] SmA 148.4[b] TGB 154.7 [0.3] N* 171.2 [3.6] I	I 165.2 [3.4] N* 152.3[b] TGB 145.6 [0.3] SmA 84.1[b] Cr
3BDC-7,8	Cr 99.8 [31.1] SmA 152.6[b] TGB 155.6 [2.1] N* 162.9 [3.9] I	I 159.7 [3.8] N* 153[b] TGB 149.8 [1.8]SmA 65[d]

[a] Peak temperatures in the DSC thermograms obtained during the first heating and cooling cycles at 5 °C min^{-1}. [b] The phase transition was observed under a polarizing microscope and was too weak to be recognized by DSC. [c] A crystal to crystal transition was observed at 120.9 [27.6]. [d] The phase freezes at 65 °C. [e] BPIII = blue phase III; BP = blue phase I/II (applicable whereever mentioned).

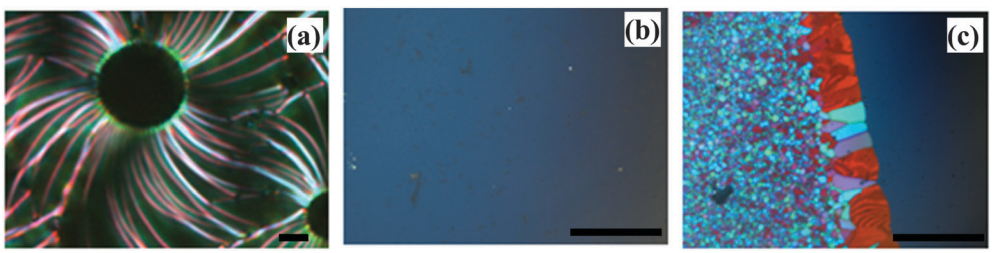

Fig. 7 (a) The filamentary texture of the TGB phase growing around the air packets of the homeotropic SmA phase (at 148 °C) of dimer **3BDC-3,8**; (b) the foggy texture of BPIII obtained at 153 °C for dimer **3BDC-4,8**; (c) the platelet texture of the cubic blue phase (either BPI or BPII) obtained at 152 °C for dimer **3BDC-4,8** (bar: 100 μm).

without any structure in it, as shown in Fig. 7b. Such a texture is reported to be seen for the BPIII phase which is an amorphous phase and has the same symmetry as the isotropic phase.[3c,24a] On further cooling, a platelet texture composed of red, green and blue plates over the foggy pattern appears at 152.7 °C (Fig. 7c); this suggests the existence of a cubic blue phase which can be either BPI or BPII.[24a] These cubic blue phases are composed of 'double twist cylinders' which represent a local structure of minimum free energy. It is may be noted here that when sheared, both high and low temperature BPs display the characteristic Grandjean planar texture of the N* phase. On lowering the temperature, the BPI/BPII phase transforms into an N* phase at 146.7 °C. Thus, the low and high temperature BPs occur over thermal ranges of 6 and 2 degrees respectively which is worth mentioning given that such phases, being highly frustrated structures, exist over a very narrow temperature interval.

The dimers **3BDC-5,8** and **3BDC-7,8** composed of 6-oxyhexanoyl and 8-oxyoctanoyl spacer, respectively, exhibit N*, TGB and SmA phases in a manner reminiscent of the thermal behavior of the first member **3BDC-3,8** of the series having an 4-oxybutanoyl (even-parity) spacer. Thus, dimers of this series having even-parity spacers behave identically with the exception of their clearing temperature which decreases with increase in spacer length. A comparison of the phase behaviour of **3BDC-5,8** with dimers **3DC-5,8** and **3RDC-5,8** shows that all of them commonly stabilize N* and TGB phases, while the occurrence and the extent of smectic behavior appear to be dependent on the nature of the chalcone segment they possess. Interestingly, the thermal behaviour of dimers **3BDC-7,8**, and **3DC-7,8** and **3RDC-7,8** is identical indicating that the dimers possessing an 8-oxyoctanoyl spacer are insensitive to variations in the structure of the chalcone mesogenic segment. As a representative case, the SmA phase formed by dimer **3BDC-7,8** was investigated by XRD. The diffractogram obtained at 145 °C showed a sharp reflection with d = 26.3 Å and a diffuse peak at wide angle with a d value of 5.1 Å (Table 2). The latter is characteristic of liquid-like order within the smectic planes. The sharp peak at 26.3 Å represents the layer thickness, with a value much less than the estimated molecular length (l) of 54 Å and thus, the d/l ratio is 0.49. This ratio is the characteristic of an intercalated SmA phase. It is appropriate to recall here that the dimer **3DC-7,8**, having the spacer and terminal tail of equal lengths, as in dimer **3BDC-7,8**, also exhibits an intercalated SmA phase.

II.2.4. Series 4 (3FDC-*n*,*m* series). Table 5 presents the LC behaviour of four dimers of the **3FDC-*n*,*m*** series where the cholesterol moiety is covalently linked to the laterally fluoro substituted chalcone core through an ω-oxyalkanoyl spacer of varying parity and length. The energy-minimized models of these dimers show that the terminal phenyl ring of the chalcone remains out of plane when compared to the co-planar organization in their non-fluoro analogues, the **3BDC-*n*,*m*** series of dimers. As we discussed at the beginning, lateral fluoro-substituents in rigid (*e.g.* biphenyl or terphenyl) cores help in reducing the melting point of the parent system.[18,19] Thus, these dimers are expected to show reduced transition temperatures. It may also be reasonable to assume that the lateral substitution of the biphenyl ring with a fluorine atom can direct the molecules to pack weakly during their self-assembly. Needless to say, such packing reduces the phase transition temperatures. As anticipated, the members of the **3FDC-*n*,*m*** series show slightly lower transition temperatures when compared to the **3BDC-*n*,*m*** series of dimers (see Table 5). Furthermore, with respect to parity of the alkylene spacer these dimers exhibit an odd–even effect in the clearing temperatures, which is in agreement with the results presented above for the other series of dimers. That is, the dimer **3FDC-3,8** having a relatively shorter spacer, the 4-oxybutanoyl (even-parity) spacer, has the highest clearing temperature followed by the dimers **3FDC-5,8** and **3FDC-7,8** having 6-oxyhexanoyl and 8-oxyoctanoyl spacers respectively. Indeed, the dimer **3FDC-4,8** exhibits the lowest clearing temperature as it contains an odd-parity (5-oxypentanoyl) spacer.

In general, all the dimers stabilize an enantiotropic N* phase. The first dimer **3FDC-3,8** additionally displays a monotropic TGBC* phase; the presence of this phase was figured out by the observation of the square grid pattern on top of the planar texture of the N* phase. In comparison with the thermal behaviour of the analogous dimer **3BDC-3,8**, compound **3FDC-3,8** disfavours the formation of a smectic phase. Notably, the next dimer **3FDC-4,8** displays BPIII over a thermal range of 4 degrees above the N* phase, which is identical to the phase behaviour of its non-fluoro analogue, the dimer **3BDC-4,8**. The dimers **3FDC-5,8** and **3FDC-7,8** display enantiotropic SmA, TGB and N* phases, while the latter compound additionally stabilizes the BPI/II. When the dimer **3FDC-7,8** was cooled gradually (0.2 °C) from the isotropic phase in the form of a thin film, a platelet texture characteristic of BPI/BPII was observed.

Table 5 Transition temperatures (°C)[a] and enthalpies (J g^{-1}) of **3FDC-*n*,8** series

Dimer **3FDC-*n*,8**	Phase sequence	
	Heating	Cooling
3FDC-3,8	Cr 132.4[b] [43.1] N* 168.8 [12.3] I	I 164.6 [12] N* 116.5[c] TGBC* 105.5[c] Cr
3FDC-4,8	Cr 127.6 [56.2] N* 139.8 [2.9] I	I 137.5 [2.4] BPIII 133.2[c] N* 87.1 [16] Cr
3FDC-5,8	Cr 110.6 [52.1] SmA 118.2 TGB 140.2 [2.4] N* 158.2 [3.6] I	I 155 [3.5] N* 136.4[c] TGB [2.3] 115[c] SmA 52.6[c,d]
3FDC-7,8	Cr 96.3 [32.9] SmA 119.5[c] TGB 121.5[c] N* 147 [4] I	I 146.8 [3.8] BP 145.2[c] N* 121[c] TGB 118[c] SmA 54.6[c] Cr

[a] Peak temperatures in the DSC thermograms obtained during the first heating and cooling cycles at 5 °C min^{-1}. [b] Additional crystal–crystal transition is observed at 110.6 [26.8]. [c] The phase transition was observed under polarizing microscope and was too weak to be recognized by DSC. [d] The mesophase freezes into the glassy state.

Upon cooling the sample further or subjecting it to mechanical stress, the platelet texture transforms to the N* phase exhibiting a brightly colored texture having oily streaks. On lowering the temperature, the transitions to TGB and SmA phases occur as established by the observation of blurred planar and focal conic textures, respectively. For the homeotropic alignment, these SmA and TGB phases displayed *pseudo*-isotropic and filamentary patterns respectively. It is appropriate to mention here that when a homeotropically aligned sample was heated at a rate of between 5–10 °C min^{-1}, the N* and SmA phases coexisted along with the TGB phase as evident from the fact that the textures corresponding to these three mesophases appeared simultaneously for a short while. Thus, dimers **3FDC-5,8** and **3FDC-7,8** commonly display enantiotropic SmA, TGB and N* phases, which is reminiscent of the phase behaviour of dimers **3BDC-5,8** and **3BDC-7,8**.

To determine the structure of the SmA phase, XRD measurements were carried out on an unoriented sample, **3FDC-7,8**, as a representative case. The results derived from the XRD diffractogram are summarized in Table 2. The 1D-intensity *vs.* 2θ profile showed a sharp peak in the low angle region and a diffuse peak in the wide-angle region with spacings 25.2 Å and 5 Å respectively. While the diffuse peak is typical of liquid-like order within the smectic planes, the sharp peak at 25.2 Å corresponds to the layer thickness and it is nearly half the value of the estimated molecular length $l \approx 53$ Å implying that dimers interdigitate between neighbouring layers. This result is in agreement with the fact that the cholesterol-based dimers such as **3DC-7,8** and **3BDC-7,8** having the spacer and terminal tail of equal lengths form an intercalated SmA phase. Recently, there was also a report where the achiral unsymmetrical dimers with an even-parity spacer exhibit an intercalated smectic phase due to the specific interaction between the unlike mesogenic segments.[30] We assume that this interaction also contributes to the formation of an intercalated SmA phase.

III. Summary

Thirty-two new optically active non-symmetric dimers belonging to four series have been synthesized and investigated for their thermal behaviour. These dimers comprise pro-mesogenic cholesterol and short bent-core chalcone, interlinked covalently through an ω-oxyalkanoyl spacer of varying length and parity. Fundamentally, these four series of compounds differing in the structure of the chalcone were prepared with the aim of comparing their thermal behaviour with that of the known dimers of identical nature, referred to as parent dimers. Our study clearly reveals the thermal behavioural differences between the new dimers and parent systems.

The dimers of the first series, which are positional isomers of the parent systems, in turn constitute four sub-series wherein cholesterol is covalently tethered to 4-*n*-alkoxy-3′-hydroxychalcone using either 4-oxybutanoyl or 5-oxypentanoyl or 6-oxyhexanoyl or 8-oxyoctanoyl spacer. Within the series, the length of the flexible terminal tail varies from *n*-octyloxy to *n*-dodecyloxy. The dimers of the first sub-series with a 4-oxybutanoyl (even-parity) spacer, in contrast to the polymesomorphic or only the smectic behaviour of parent analogues, exhibit only the N* phase; this indicates the importance of the position at which the cholesteryloxycarbonyl-*n*-alkane is attached to the chalcone in determining their phase behaviour. Within this series, the variation of the length of the terminal tail seems to have almost no effect on the I–N* phase transition temperature. The dimers of the second sub-series with an odd-parity (5-oxypentanoyl) spacer, contrary to expectation, did not show any LC phase; this can be attributed to the pronounced bent conformation and thus reduced shape anisotropy of the molecules. The dimers of the third sub-series having a 6-oxyhexanoyl (even-parity) spacer stabilize an enantiotropic N* phase; except for the dimer possessing an *n*-decyloxy tail, all of them also display a monotropic TGB/TGBC* phase. Within the series, the increase in the length of terminal chain appears not to have much effect on the Cr–N*, N*–I or I–N* phase transition temperatures; instead, it determines the type of frustrated phase to be formed. The first two dimers possessing *n*-octyloxy and *n*-nonyloxy tails display TGB phases (which may have either SmA or SmC slabs), while the other two compounds with *n*-undecyloxy and *n*-dodecyloxy tails stabilize TGBC* phases. Moreover, the alternation of the N*–TGB or N*–TGBC* transition temperature (during cooling) as a function of the number of carbon atoms in the terminal chain occurs. In the dimers of the fourth sub-series in which the cholesterol and chalcone entities are joined covalently through an 8-oxyoctanoyl spacer, the length of the terminal tail influences the phase behaviour. The dimers with *n*-octyloxy to *n*-decyloxy tails stabilize N*, TGB and SmA phases while compounds comprising *n*-undecyloxy and *n*-dodecyloxy chains display a sequence involving a transition from the N* to TGB/TGBC* phase; here also there are marginal transition temperature alternations as a function of the length of the terminal chain persists. The XRD study on the SmA phase of dimer having *n*-octyloxy tail confirmed the intercalated organization of the molecules within the phase. Most importantly, these four series of compounds display a different behaviour compared to parent systems clearly indicating the dependence of phase transitional properties of cholesterol-based dimers on the nature of the rod-like (non-cholesteryl) mesogen; the study also confirms a dramatic dependence of their transitional properties on the length and parity of the spacer.

In the second series, as compared to the parent systems or the members of the first series, the chalcone (α,β-unsaturated ketone) linkage is reversed imparting an extended linear conformation to the molecules. It is a rather short series, where the length of the terminal tail *viz.*, *n*-octyloxy, is kept constant while the length and parity of the spacer is varied. Three dimers having an even-parity spacer exhibit mesophases whereas the compound with an odd-parity (5-oxypentanoyl) spacer is non-mesomorphic. The dimer with a 4-oxybutanoyl spacer displays SmA and SmC* phases for which the monolayer and tilted monolayer arrangements of the molecules were evidenced by XRD studies. The compound having a 6-oxyhexanoyl spacer exhibits the sequence N*–TGB–SmA–SmC*, while in the dimer with an 8-oxyoctanoyl spacer, the SmC* phase is suppressed.

The dimers belonging to the third series are different from those of the parent series or the two series of materials described above. That is, they possess an elongated chalcone where one of the aryl rings is substituted with a 4-*n*-octyloxybiphenyl instead of a phenyl ring. Interestingly, all of them are mesomorphic; stabilization of BPIII, BPI/II and N* phases by the dimer possessing an odd-parity (5-oxypentanoyl) spacer is noteworthy in view of the fact that the compounds of the other series with an analogous spacer are crystalline. The other three dimers having 4-oxybutanoyl or 6-oxyhexanoyl or 8-oxyoctanoyl spacers exhibit N*, TGB and SmA phases. The occurrence of the intercalated SmA phase for the dimer consisting of an 8-oxyoctanoyl spacer was established by XRD measurements. The increase in the spacer length seems to reduce the Cr–SmA/N*, N*–I or I–N* transition temperatures. In general, the thermal behaviour of these compounds agrees with that of the parent dimers.

The fourth series of dimers, which are the fluoro analogues of dimers of the third series, display mesomorphic behavior with the expected lower transition temperatures. In this series also, the dimer with an odd-parity spacer is mesomorphic exhibiting BP and N* phases. For the members with even-parity spacers, the number of mesophases increases on lengthening the spacer; the dimers with 4-oxybutanoyl, 6-oxyhexanoyl and 8-oxyoctanoyl spacers show respectively the sequences: N*–TGBC*, N*–TGB–SmA and BP–N*–TGB–SmA.

In essence, the study clearly illustrates the complex interplay of the different molecular sub-units of the dimers in stabilizing mesophases such as blue phase(s), chiral nematic, twist grain boundary, smectic A and chiral smectic C phases.

Acknowledgements

CVY sincerely thanks the Science and Engineering Board (SERB), DST, Govt. of India for funding this work through the project No. SR/S1/OC-04/2012.

References

1 (*a*) S. Chandrasekhar, *Liquid Crystals*, Cambridge University Press, New York, 2nd edn 1994; (*b*) P. G. De Gennes and J. Prost, *The Physics of Liquid Crystals*, Oxford Science Publication, Oxford, 1993; (*c*) *Handbook of Liquid Crystals: Fundamentals*, ed. J. W. Goodby, P. J. Collings, T. Kato, C. Tschierske, H. Gleeson and P. Raynes, Wiley-VCH, Weinheim, Germany, 2014, vol. 1; (*d*) J. W. Goodby, I. M. Saez, S. J. Cowling, V. Görtz, M. Draper, A. W. Hall, S. Sia, G. Cosquer, S.-E. Lee and E. P. Raynes, *Angew. Chem., Int. Ed.*, 2008, **47**, 2754; (*e*) T. Geelhaar, K. Griesar and B. Reckmann, *Angew. Chem., Int. Ed.*, 2013, **52**, 8798; (*f*) C. Tschierske, *Angew. Chem., Int. Ed.*, 2013, **52**, 8828.

2 F. Renitzer, *Monatsh. Chem.*, 1888, **9**, 421.

3 (*a*) I. Sage, in *Liquid Crystals: Applications and Uses*, ed. B. Bahadur, World Scientific, Singapore, 1992, ch. 20, vol. 3; (*b*) *Nanoscience with Liquid Crystals: From Self-Organized Nanostructures to Applications*, ed. Q. Li, Springer, 2014; (*c*) *Liquid Crystals Beyond Displays: Chemistry, Physics, and Applications*, ed. Q. Li, John Wiley & Sons, 2012; (*d*) E.-K. Fleischmann and R. Zentel, *Angew. Chem., Int. Ed.*, 2013, **52**, 8810; (*e*) M. Bremer, P. Kirsch, M. Klasen-Memmer and K. Tarumi, *Angew. Chem., Int. Ed.*, 2013, **52**, 8880.

4 (*a*) S. R. Renn and T. C. Lubensky, *Phys. Rev. A: At., Mol., Opt. Phys.*, 1988, **38**, 2132; (*b*) P. G. de Gennes, *Solid State Commun.*, 1972, **10**, 753; (*c*) H.-S. Kitzerow and C. Bahr, *Chirality in Liquid Crystals*, Springer-Verlag, Inc., New York, 2001; (*d*) J. W. Goodby, *Curr. Opin. Colloid Interface Sci.*, 2001, **7**, 326; (*e*) J. W. Goodby, M. A. Waugh, S. M. Stein, E. Chin, R. Pindak and J. S. Patel, *Nature*, 1989, **337**, 449; (*f*) J. W. Goodby, M. A. Waugh, S. M. Stein, E. Chin, R. Pindak and J. S. Patel, *J. Am. Chem. Soc.*, 1989, **111**, 8119; (*g*) J. W. Goodby, in *Structure and Bonding: Liquid Crystals II*, ed. D. M. P. Mingos, Springer-Verlag, Berlin, 1999, p. 83.

5 (*a*) S. T. Lagerwall, in *Ferroelectric and Antiferroelectric Liquid Crystals*, ed. S. T. Lagerwall, Wiley-VCH, Weinheim, Germany, 1999; (*b*) D. M. Walba, *Science*, 1995, **270**, 250; (*c*) S. Garoff and R. Meyer, *Phys. Rev. Lett.*, 1977, **38**, 848–851; (*d*) S. T. Lagerwall, M. Matuszcyk, P. Rodhe and L. Odma, in *The Optics of Thermotropic Liquid Crystals*, ed. S. J. Elston and J. R. Sambles, Taylor and Francis, London, 1998.

6 (*a*) Z. Ge, S. Gauza, M. Jiao, H. Xianyu and S. T. Wu, *Appl. Phys. Lett.*, 2009, **94**, 101104; (*b*) J. Yan, L. Rao, M. Jiao, Y. Li, H. C. Cheng and S. T. Wu, *J. Mater. Chem.*, 2011, **21**, 7870; (*c*) Y. H. Lin, H. S. Chen and T. H. Chiang, *J. Soc. Inf. Disp.*, 2012, **20**, 333; (*d*) J. Yan, S. T. Wu, K. L. Cheng and J. W. Shiu, *Appl. Phys. Lett.*, 2013, **102**, 081102; (*e*) Y. Chen and S. T. Wu, *Appl. Phys. Lett.*, 2013, **102**, 171110; (*f*) H. J. Coles and S. Morris, *Nat. Photonics*, 2010, **4**, 676; (*g*) W. Cao, A. Munoz, P. Palffy-Muhoray and B. Taheri, *Nat. Mater.*, 2002, **1**, 111; (*h*) F. Castles, F. V. Day, S. M. Morris, D.-H. Ko, D. J. Gardiner, M. M. Qasim, S. Nosheen, P. J. W. Hands, S. S. Choi, R. H. Friend and H. J. Coles, *Nat. Mater.*, 2012, **11**, 599; (*i*) T.-H. Lin, Y. Li, C.-T. Wang, H.-C. Jau, C.-W. Chen, C.-C. Li, H. Krishna Bisoyi, T. J. Bunning and Q. Li, *Adv. Mater.*, 2013, **25**, 5050; (*j*) H. J. Coles and M. N. Pivnenko, *Nature*, 2005, **436**, 997; (*k*) H. Kikuchi, M. Yokota, Y. Hisakado, H. Yang and T. Kajiyama, *Nat. Mater.*, 2002, **1**, 64.

7 (*a*) C. T. Imrie, in *Structure and Bonding – Liquid Crystals, II*, ed. D. M. P. Mingos, Springer-Verlag, 1999, p. 149; (*b*) C. T. Imrie and P. A. Henderson, *Curr. Opin. Colloid Interface Sci.*, 2002, **7**, 298; (*c*) C. T. Imrie and P. A. Henderson, *Chem. Soc. Rev.*, 2007, **36**, 2096; (*d*) C. T. Imrie and G. R. Luckhurst, in *Handbook of liquid crystals*, ed. D. Demus, J. W. Goodby, G. W. Gray, H.-W. Spiess and V. Vill, Weiley-VCH, Germany, 1998, vol. 2B, part – III, p. 799.

8 V. Borshch, Y.-K. Kim, J. Xiang, M. Gao, A. Jaklil, V. P. Panov, J. K. Vij, C. T. Imrie, M. G. Tamba, G. H. Mehl and O. D. Lavrentovich, *Nat. Commun.*, 2013, **4**, 2635.

9 (*a*) D. S. Shankar Rao, S. Krishna Prasad, V. N. Raja, C. V. Yelamaggad and S. A. Nagamani, *Phys. Rev. Lett.*, 2001, **87**, 085504; (*b*) C. V. Yelamaggad, M. Mathews, T. Fujita and N. Iyi, *Liq. Cryst.*, 2003, **30**, 1079.

10 (*a*) C. V. Yelamaggad, G. Shanker, U. S. Hiremath and S. K. Prasad, *J. Mater. Chem.*, 2008, **18**, 2927 and the references cited therein; (*b*) C. T. Imrie, P. A. Henderson and G.-Y. Yeap, *Liq. Cryst.*, 2009, **36**, 755.

11 (*a*) F. Hardouin, M. F. Achard, J.-I. Jin, J. W. Shin and Y. K. Yun, *J. Phys. II*, 1994, **4**, 627; (*b*) F. Hardouin, M. F. Achard, J.-I. Jin and Y. K. Yun, *J. Phys. II*, 1995, **5**, 927; (*c*) F. Hardouin, M. F. Achard, J.-I. Jin, Y. K. Yun and S. J. Chung, *Eur. Phys. J. B*, 1998, **1**, 47.

12 (*a*) S.-W. Cha, J.-I. Jin, M. Laguerre, M. F. Achard and F. Hardouin, *Liq. Cryst.*, 1999, **26**, 1325; (*b*) F. Hardouin, M. F. Achard, M. Laguerre, J.-I. Jin and D. H. Ko, *Liq. Cryst.*, 1999, **26**, 589; (*c*) D. W. Lee, J.-I. Jin, M. Laguerre, M. F. Achard and F. Hardouin, *Liq. Cryst.*, 2000, **27**, 145; (*d*) S.-W. Cha, J.-I. Jin, M. F. Achard and F. Hardouin, *Liq. Cryst.*, 2002, **29**, 755; (*e*) J.-W. Lee, Y. Park, J.-I. Jin, M. F. Achard and F. Hardouin, *J. Mater. Chem.*, 2003, **13**, 1367; (*f*) K.-N. Kim, E.-D. Do, Y.-W. Kwon and J.-I. Jin, *Liq. Cryst.*, 2005, **32**, 229.

13 (*a*) A. T. M. Marcelis, A. Koudijs and E. J. R. Sudholter, *Recl. Trav. Chim. Pays-Bas*, 1994, **113**, 524; (*b*) A. T. M. Marcelis, A. Koudijs and E. J. R. Sudholter, *Liq. Cryst.*, 1995, **18**, 843.

14 (*a*) A. T. M. Marcelis, A. Koudijs, E. A. Klop and E. J. R. Sudholter, *Liq. Cryst.*, 2001, **28**, 881 and references cited therein; (*b*) A. T. M. Marcelis, A. Koudijs, Z. Karczmarzyk and E. J. R. Sudholter, *Liq. Cryst.*, 2003, **30**, 1357.

15 (*a*) C. V. Yelamaggad, A. Srikrishna, D. S. Shankar Rao and S. K. Prasad, *Liq. Cryst.*, 1999, **26**, 1547; (*b*) C. V. Yelamaggad, *Mol. Cryst. Liq. Cryst.*, 1999, **326**, 149; (*c*) C. V. Yelamaggad, S. A. Nagamani, D. S. Shankar Rao, S. K. Prasad and U. S. Hiremath, *Mol. Cryst. Liq. Cryst.*, 2001, **363**, 1; (*d*) C. V. Yelamaggad, U. S. Hiremath and D. S. Shankar Rao, *Liq. Cryst.*, 2001, **28**, 351; (*e*) C. V. Yelamaggad, S. A. Nagamani, U. S. Hiremath and G. G. Nair, *Liq. Cryst.*, 2001, **28**, 1009; (*f*) C. V. Yelamaggad and M. Mathews, *Liq. Cryst.*, 2003, **30**, 125; (*g*) C. V. Yelamaggad, I. Shashikala, U. S. Hiremath, D. S. Shankar Rao and S. Krishna Prasad, *Liq. Cryst.*, 2007, **34**, 153; (*h*) C. V. Yelamaggad, A. S. Achalkumar, N. L. Bonde and A. K. Prajapati, *Chem. Mater.*, 2006, **18**, 1076; (*i*) C. V. Yelamaggad, A. S. Achalkumar, N. L. Bonde, A. K. Prajapati, D. S. S. Rao and S. K. Prasad, *Chem. Mater.*, 2007, **19**, 2463; (*j*) K. C. Majumdar, P. K. Shyam, D. S. S. Rao and S. K. Prasad, *J. Mater. Chem.*, 2011, **21**, 556; (*k*) A. S. Pandey, R. Dhara, A. S. Achalkumar and C. V. Yelamaggad, *Liq. Cryst.*, 2011, **38**, 775; (*l*) G. Shanker and C. V. Yelamaggad, *New J. Chem.*, 2012, **36**, 918.

16 G. S. Lim, B. M. Jung, S. J. Lee, H. H. Song, C. Kim and J. Y. Chang, *Chem. Mater.*, 2007, **19**, 460 and references cited therein.

17 (*a*) W. Tam, B. Gucrim, J. C. Calabreso and S. U. Sterenson, *Chem. Phys. Lett.*, 1989, **154**, 93; (*b*) J. Indira, P. P. Karat and B. K. Sarojini, *J. Cryst. Growth*, 2002, **242**, 209; (*c*) X. T. Tao, T. Watanabe, K. Kono, T. Deguchi, M. Nakayama and S. Miyata, *Chem. Mater.*, 1996, **8**, 1326.

18 (*a*) V. Bezborodoc, R. Dabrowski, J. Dziaduszek, K. Czuprynski and Z. Raszewski, *Liq. Cryst.*, 2006, **33**, 1487; (*b*) M. Hird and K. J. Toyne, *Mol. Cryst. Liq. Cryst.*, 1998, **323**, 1; (*c*) T. Hiyama, *Organoflourine Compounds, Chemistry and Applications*, Springer-Verlag Berlin Heidelberg, New York, 2000.

19 (*a*) G. W. Gray, M. Hird, D. Lacey and K. J. Toyne, *J. Chem. Soc., Perkin Trans. 2*, 1989, 2041; (*b*) M. E. Gledenning, J. W. Goodby, M. Hird and K. J. Toyne, *J. Chem. Soc., Perkin Trans. 2*, 1999, 481; (*c*) M. E. Gledenning, J. W. Goodby, M. Hird, D. Lacey and K. J. Toyne, *J. Chem. Soc., Perkin Trans. 2*, 2000, 27; (*d*) M. Hird, J. W. Goodby and K. J. Toyne, *Proc. SPIE.*, 2000, **3955**, 15; (*e*) W.-K. Lee, K.-N. Kim, M. F. Achard and J.-I. Jin, *J. Mater. Chem.*, 2006, **16**, 2289.

20 I. W. Hamley, V. Castelletto, P. Parras, Z. B. Lu, C. T. Imrie and T. Itoh, *Soft Matter*, 2005, **1**, 355 and references cited therein.

21 V. Surendranath, *Mol. Cryst. Liq. Cryst.*, 1999, **332**, 135.

22 N. K. Chudgar and S. N. Shah, *Liq. Cryst.*, 1989, **4**, 661.

23 S.-W. Cha, J.-I. Jin, M. F. Achard and F. Hardouin, *Liq. Cryst.*, 2002, **29**, 755.

24 (*a*) I. Dierking, *Textures of Liquid Crystals*, Wiley-VCH Verlag GmBH & KGaA, Weinheim, 2003; (*b*) I. Dierking and S. T. Lagerwall, *Liq. Cryst.*, 1999, **26**, 83.

25 Y. Galerne, *Eur. Phys. J. E: Soft Matter Biol. Phys.*, 2000, **3**, 355.

26 C. V. Yelamaggad, U. S. Hiremath, D. S. Shankar Rao and S. K. Prasad, *Chem. Commun.*, 2000, 57.

27 C. V. Yelamaggad, A. S. Nagamani, U. S. Hiremath, D. S. Shankar Rao and S. K. Prasad, *Liq. Cryst.*, 2001, **28**, 1581.

28 C. V. Yelamaggad, S. A. Nagamani, U. S. Hiremath, D. S. Shankar Rao and S. K. Prasad, *J. Chem. Res.*, 2001, 493.

29 W.-K. Lee, K.-N. Kim, M. F. Achard and J.-I. Jin, *J. Mater. Chem.*, 2006, **16**, 2289 and references cited therein.

30 G.-Y. Yeap, T.-C. Hng, S.-Y. Yeap, E. Gorecka, M. M. Ito, K. Ueno, M. Okamoto, W. Ahmad, K. Mahmood and C. T. Imrie, *Liq. Cryst.*, 2009, **36**, 1431.

